Astron. Astrophys. 269, 119–127 (1993)

ASTRONOMY AND ASTROPHYSICS

Angular source size measurements and interstellar scattering at 103 MHz using interplanetary scintillation

P. Janardhan★ and S.K. Alurkar

Physical Research Laboratory, Radio Astronomy Division, Navrangpura, Ahmedabad - 380009, India

Received May 27, accepted August 6, 1992

Abstract. Data obtained between 1984 and 1987, using a radio telescope (R.T) with a 10000 m^2 dipole array operating at 103 MHz, was used to determine the angular diameters of fourteen strongly scintillating radio sources. The method used exploited the technique of interplanetary scintillation (IPS), wherein the systematic variation of scintillation index (m) with solar elongation (ε) was used as a unique indicator of the source size. The method has been used before but these are the first measurements at 103 MHz. These values were then used in conjunction with similar available measurements at 151.5 MHz to determine the contribution of interstellar scattering (ISS) to source broadening at 103 MHz. Enhanced scattering due to ISS in the plane of the galaxy has been confirmed.

Key words: interplanetary scintillation – compact radio source – angular diameters – interstellar scattering

1. Introduction

IPS observations at meter wavelengths offer a useful method of studying the angular diameters of compact radio sources. Ideally, information about the squared magnitude of the visibility function can be determined from a complete set of IPS spectra obtained in strong scattering, with each observation being a cut across the visibility function in the direction of the solar wind velocity vector. A knowledge of the solar wind speed will also be required so as to be able to normalize each IPS spectrum. A large number of such observations, each representing a cut across the visibility function in a different direction, could thus be used to get a complete picture of the source with only the phase information being absent in the complex visibility function. The reason why such a method is not feasible is because many sources, due to their positions, do not approach close enough to the sun to be in the strong scattering regime and many sources which do pass close to the sun, do so for very short periods. Also the scintillation index (rms flux/mean source flux) decreases rapidly as the source visibility function begins to cut off the IPS spectrum, causing many sources to be unobservable in this period. Radio interference from the sun can also effectively wipe out meaningful observations in a large number of cases. Moreover, the source visibility function depends upon the intrinsic character of the source and the scattering properties of the plasma along the line of sight to the source and it is in general difficult to separate the two effects. Only in the case of very compact sourced like pulsars, which can be taken to be ideal "point sources", the observed angular diameter will be completely dominated by scattering and the form of the visibility function can be determined by the shape of the spectrum of electron density irregularities in the interstellar medium. The bulk of previous scattering experiments in the Galaxy have been made mostly by pulsar pulse-broadening and decorrelation measurements (Cordes et al. 1985, 1991; Alurkar et al. 1986).

One method of measuring angular diameters using IPS would be to compare the width of the power spectrum in weak scattering (Cohen et al. 1967; Rao et al. 1974) or strong scattering (Kaufmann 1976) with that of a point source. The recent method of fitting model IPS power spectra (Manoharan & Ananthakrishnan 1990) to determine solar wind velocities can also be used to estimate angular diameters of radio sources.

Due to its simplicity, the Gaussian model visibility function has been widely used in determining radio source structure. But in this case the true visibility function is severely limited causing both low frequency VLBI and IPS techniques to suffer. Hence the absence of an *a priori* knowledge of the true brightness distribution causes one to assume circular symmetry and approximate the real source profile by a Gaussian having a characteristic width to $1/e$, leading to the calculation of the source diameter.

2. The method of source diameter measurements using IPS

In the present study the angular diameters of fourteen radio sources were calculated using the assumption of a

Send offprint requests to: P. Janardhan

★ Now at: Radio Astronomy Centre (TIFR) P.O. Box 8; Udhagamandlam-643001 India.

Gaussian brightness distribution and observations of the variation of scintillation index (m) with solar elongation (ε). The assumption of a circularly symmetric Gaussian model for the compact component of a radio source is a useful first approximation and it has been shown (Little & Hewish 1966) that provided the source model does not contain more than one component or is not greatly elongated in a particular direction the method yields the same result and is insensitive to the type of model used. The angular size measurements, though, are all subject to errors due to broadening by ISS which, in general, causes the true source brightness distribution to tend towards a symmetrical Gaussian model. IPS measurements of angular diameters based on the Gaussian model have been carried out (Harris et al. 1970; Readhead & Hewish 1972; Cohen & Cronyn 1974; Duffett-Smith & Readhead 1976) and used to derive an approximate formula for the interstellar scattering angle (Θ_S) at a given frequency.

Essentially the method of determining source sizes by using IPS is based on the systematic variation of m of a compact radio source with ε. At large ε the scattering is weak and m is small, but as one approaches the Sun m gradually increases reaching a peak value at 103 MHz at approximately 30°elongation and then falls off again, in the strong scattering regime, due to blurring across the finite receiver bandwidth and finite source size. Although m varies from day-to-day, depending upon the conditions prevailing in the interplanetary medium (IPM), a large number of observations of a given radio source over a range of ε from about 10–90° can be used to determine the mean behaviour of m as a function of ε by fitting the data points by a polynomial.

The scintillation index depends upon the observing frequency (f), the solar elongation (ε), the brightness distribution of the source $B(\theta, \phi)$ and the prevailing conditions in the IPM. If one assumes a model for the IPM (Readhead 1971; Marians 1975b) m can be calculated in either the weak scattering regime, where it increases with decreasing ε or the strong scattering regime, where it decreases with decreasing ε. Close to the turnover, however, m is calculated by interpolation since no analytical formulation is valid in this region. The model used in this study assumes a Gaussian spectrum of electron density irregularities given by (Readhead et al. 1978; henceforth referred to as RKH) to calculate the variation of m with ε. Figure 1 shows the calculated curves of m vs. ε at 103 MHz based on a composite IPM model by Kemp (1979).

Under the assumption that the true source profile is a Gaussian with circular symmetry, the brightness distribution (B (θ, ϕ) loses its ϕ dependence and can simply be written as $B(\Theta)$, where Θ is the equivalent Gaussian diameter of the source. A single value of the scintillating flux ΔS cannot be used to determine Θ. Current models of the IPM cannot pinpoint the turnover in the m vs. ε curves and at the same time provide a good fit to data at large elongations (Purvis 1981). The best estimate of the source

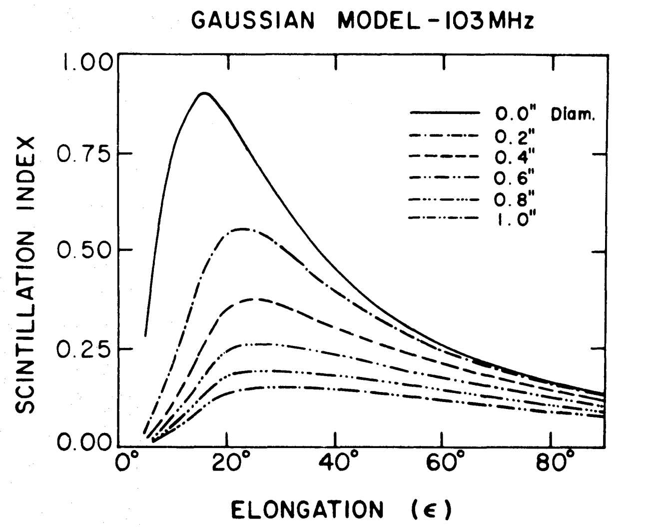

Fig. 1. Shows the calculated curves of scintillation index (m) vs. solar elongation (ε) using a composite model of the interplanetary medium (Kemp 1979). Each curve is unique for a given source size

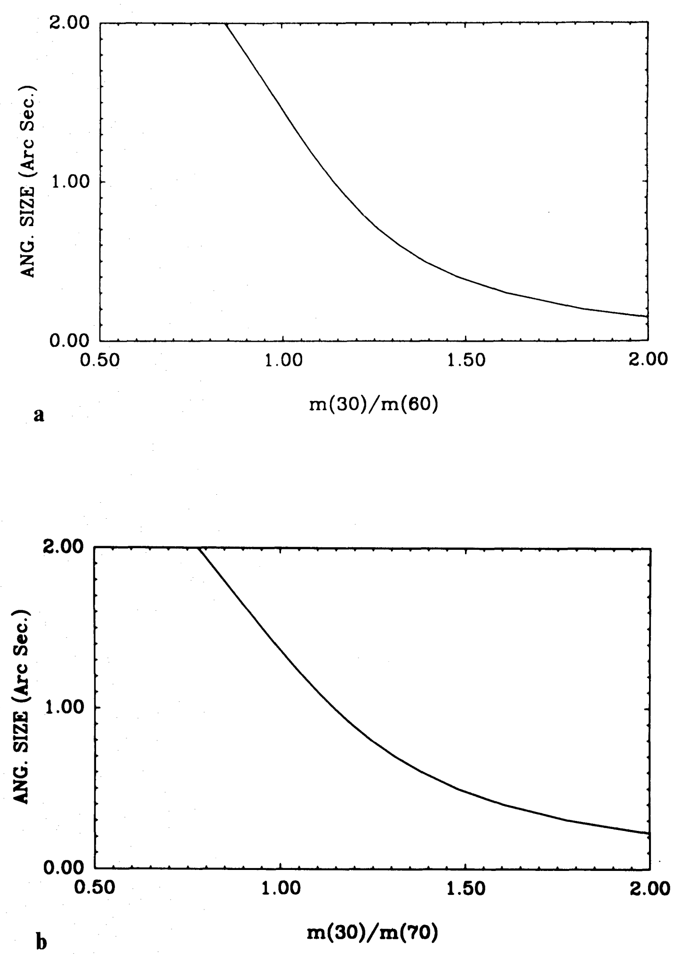

Fig. 2a–b. Shows the variation of angular size (Θ) with changing scintillating index ratio ($\mathscr{R}$). The value of ε_2 is 60° in Fig. 2a while it is 70° in Fig. 2b

size is obtained by the slope of the m vs. ε curve (Readhead 1971), which is a unique indicator of Θ. In practice, m is measured for a given source over a wide range of ε and the ratio of the scintillation index at two widely separated elongations is found. The ratio, $\mathscr{R}$ for known elongations is a function of Θ only and there now exists a one-to-one correspondence between Θ and $\mathscr{R}$. Once $\mathscr{R}$ is determined by observations, Θ can be determined easily. Essentially:

$$\mathscr{R}=\frac{\Delta S_1}{\Delta S_2}=\frac{m(\Theta\varepsilon_1)}{m(\Theta\varepsilon_2)}=F(\Theta). \tag{1}$$

Figure 2a, 2b shows plots of Θ vs. $\mathscr{R}$. The curves were obtained using the calculated values of m at 103 MHz. Thus, all that is now required is to observe a given source over a wide range of ε and determine $\mathscr{R}$ after fitting the observed data points with a 3rd order polynomial. Knowing $\mathscr{R}$ the value of Θ can easily be found. Since many of the sources were not observed at Thaltej, near Ahmedabad much beyond 60°, it was necessary to use both the curves 2a, b for determining Θ depending on whether the observations extended beyond 60° or 70° elongation.

3. The IPS telescope and observations

The observations were carried out with the 10 000 m^2 dipole array R.T at Thaltej, near Ahmedabad, India and Fig. 3 shows a plot of the positions of the various scintillating sources seen by the Thaltej telescope in ecliptic coordinates. This antenna is filled aperture phased array, made up of 2048 fullwave dipoles. The array is divided into two halves viz. the North and South. Each half comprises 32 transmission lines each loaded with 32 dipoles, polarized horizontally in the N–S direction to form a correlation type interferometer observing sources at meridian transit. Thirty two beams are formed by each half of the array using a beam forming network called the Butler matrix, which is essentially the analogue equivalent of a Fast Fourier Transform. These beams are deployed in declination and are each 1.8° N–S × 3.6° E–W and cover ±30° of

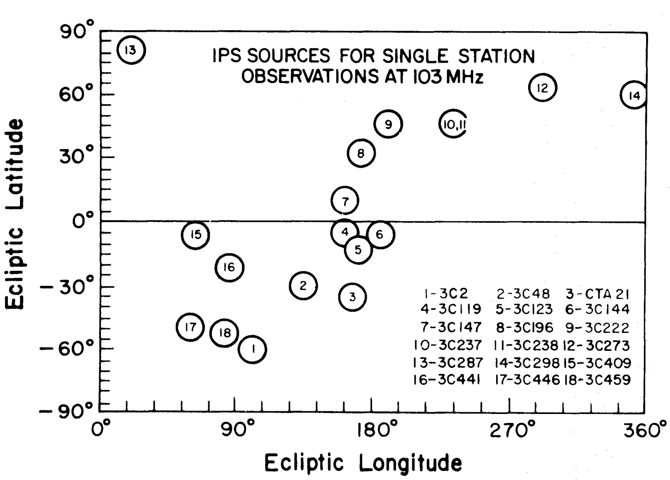

Fig. 3. Shows the positions, in ecliptic coordinates, of the scintillating sources observable from Thaltej

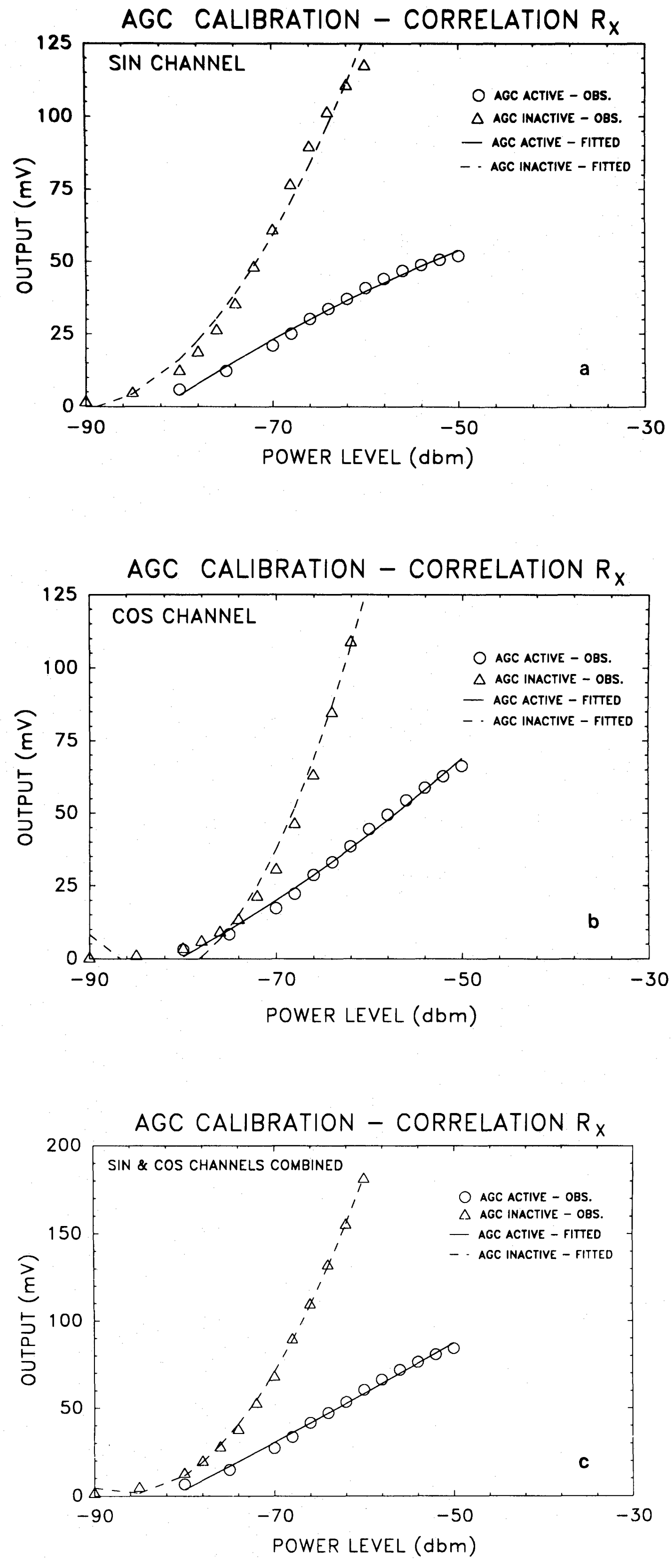

Fig. 4a–c. Shows the behaviour of the square law detector output with and without the automatic gain control (AGC) active, for changing input power levels. The open triangles and circles are measurements while the solid and broken lines are second order polynomial fits. **a** and **b** represent the sin and cos channels while **c** shows the effective output given by $\sqrt{\sin^2(\text{deflection})+\cos^2(\text{deflection})}$

declination centered on the zenith. A pair of identical beams is connected, during each observation, to a correlation type receiver which yields Sine and Cosine quadrature outputs. Each of the two receiver channels thus formed are fed through two 30 MHz intermediate frequency (IF) amplifiers with an average half power bandwidth of 4.5 MHz. The outputs of these high gain (80 db) IF amplifiers are maintained at a constant level within about 1 db using an automatic gain control (AGC) having a time constant of about 3 s. The characteristics of the square-law detector are such that the AGC becomes effective without even the antenna being connected. The square-law detector diodes are selected for similarity and are connected so that the voltage remains within the square-law range of about 10 mV to 70 mV. The AGC is so adjusted that with the antenna array connected and a source in the beam the square-law output remains below 45 mV. It was found that the AGC time constant, being so close to the time scale of IPS, was causing a reduction in the sensitivity. To allow for this the data had to be corrected for the effects of the AGC. Figure 4a, b shows the behaviour of the sin and cos channels with and without the AGC in operation, while Fig. 4c plots the same ouput using the effective deflection given by $(\sin^2+\cos^2)^{1/2}$. The rapidly changing intensity fluctuations are picked up by a device, called the scintillometer, which passes frequencies in the range 0.04–5.0 Hz and whose output is proportional to the square of the scintillating flux of the source (Duffett-Smith 1976).

4. Measurement of scintillation index

The scintillation indices were derived from the measured deflection on the sin, cos and scintillometer channels of the chart recorder after appropriate calibration. If v_1 denotes the output voltage of the receiver and v_2 the output voltage of the scintillometer, then v_1 is given by

$$v_1 = CT_1\bar{S}$$

Where C is some constant of proportionality, T_1 is the antenna temperature and $\bar{S}$ is the mean source flux. Similarly, since the scintillometer is a square-law device and is sensitive only to the scintillating flux ΔS,

$$v_2 = K(CT_1)^2\,(\Delta S)^2$$

where K is another constant. Using these two relations one gets,

$$\Delta S^2 = \frac{v_2\bar{S}^2}{Kv_1^2}. \quad (2)$$

Here the only quantity that has to be determined is the constant K. The mean source flux $\bar{S}$ was taken from the 81.5 MHz catalogue (Readhead & Hewish 1974) and scaled to 103 MHz using the relation $S_f = f^{-0.75}$, (Readhead & Hewish 1974) where S_f is the flux at a frequency f. The constant K was determined by appropriately calibrating the scintillometer.

Using the value of K obtained from the scintillometer calibration procedure and the measured deflections of the sin, cos and scintillometer channels and scintillation index can be determined after correcting the deflections for the effects of the AGC using the curves in Fig. 4a–c. Figures 5a–n shows the values of m obtained for various sources plotted as a function of ε. The data available from all the years between mid–1984 and end of 1987 were used and the data points were then fitted by a 3rd order polynomial. Each open circle in the figure represents the mean value of all data falling within a 1° bin of ε. The solid line, shown separately below each set of observations, represents, a third order polynomial fit with the filled circles representing the mean values in each 10° bin. Shown also is a

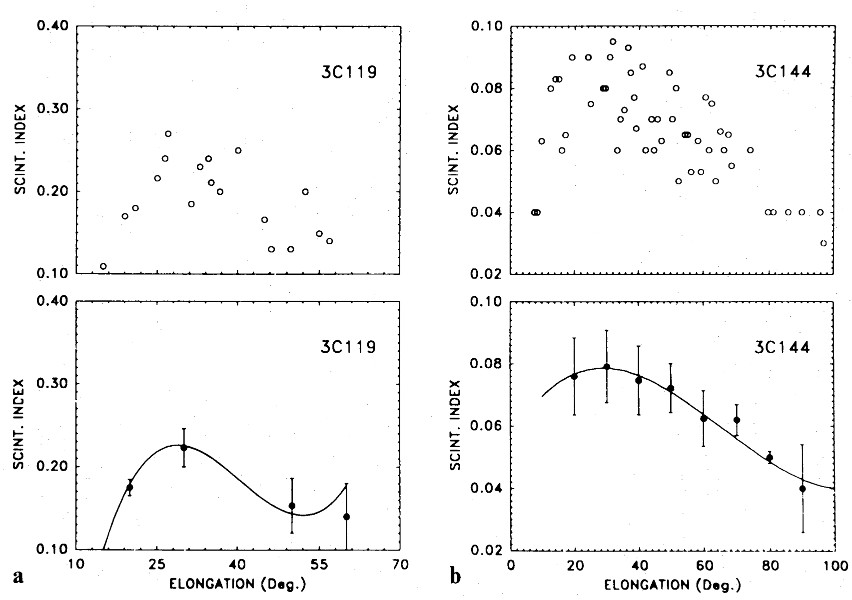

Fig. 5a–n. Shows the observations (upper boxes) of m as a function of ε for each of the fourteen sources. Third order polynomial fits (lower boxes) with filled circles representing mean values in each 10° bin and corresponding standard error bars are also shown. Each open circle represents the mean of all values in a 1° bin. The sources are respectively 3C 119, 3C 144, 3C 147, 3C 48, 3C 196, CTA 21, 3C 222, 3C 237, 3C 446, 3C 459, 3C 2, 3C 298, 3C 273 and 3C 287

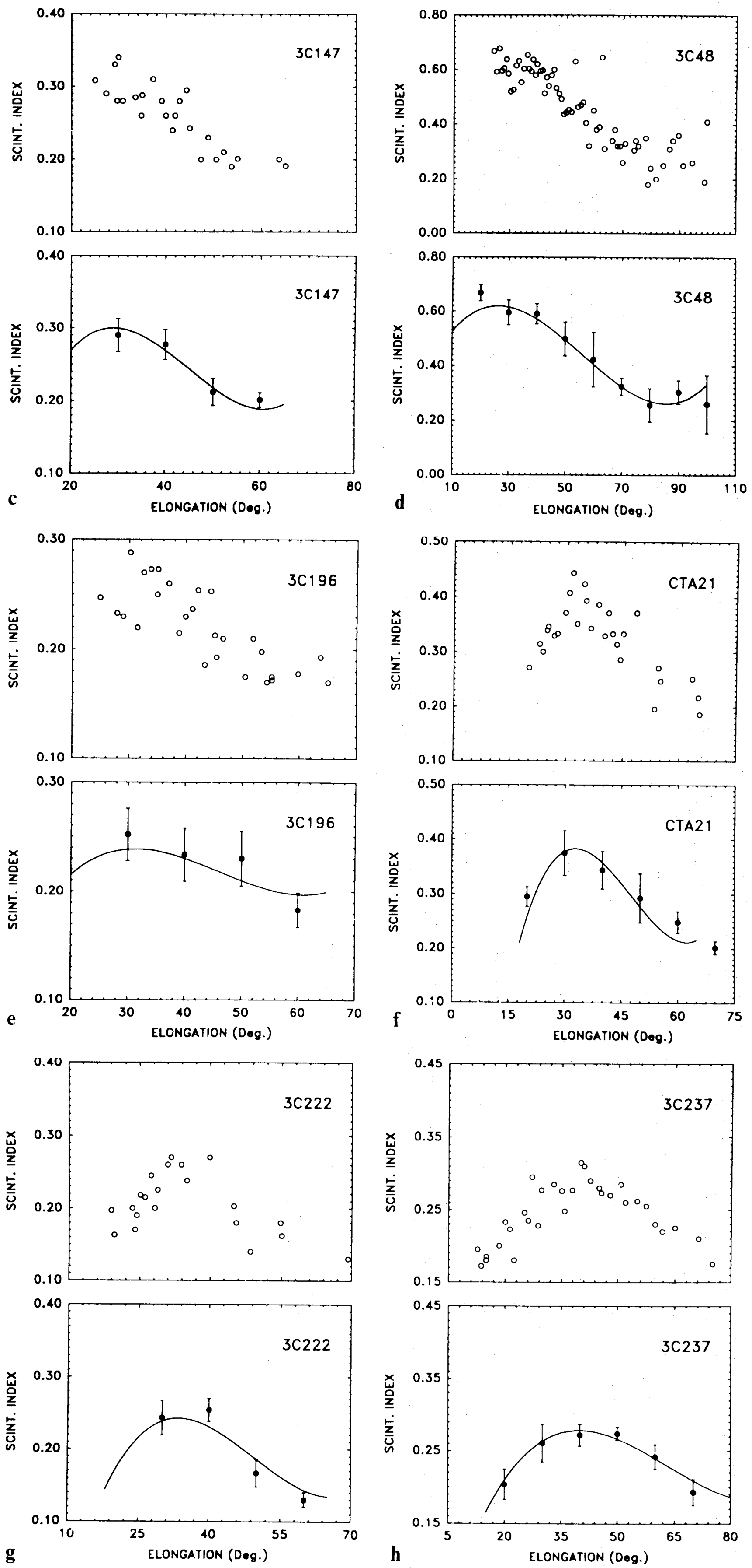

Fig. 5 (continued)

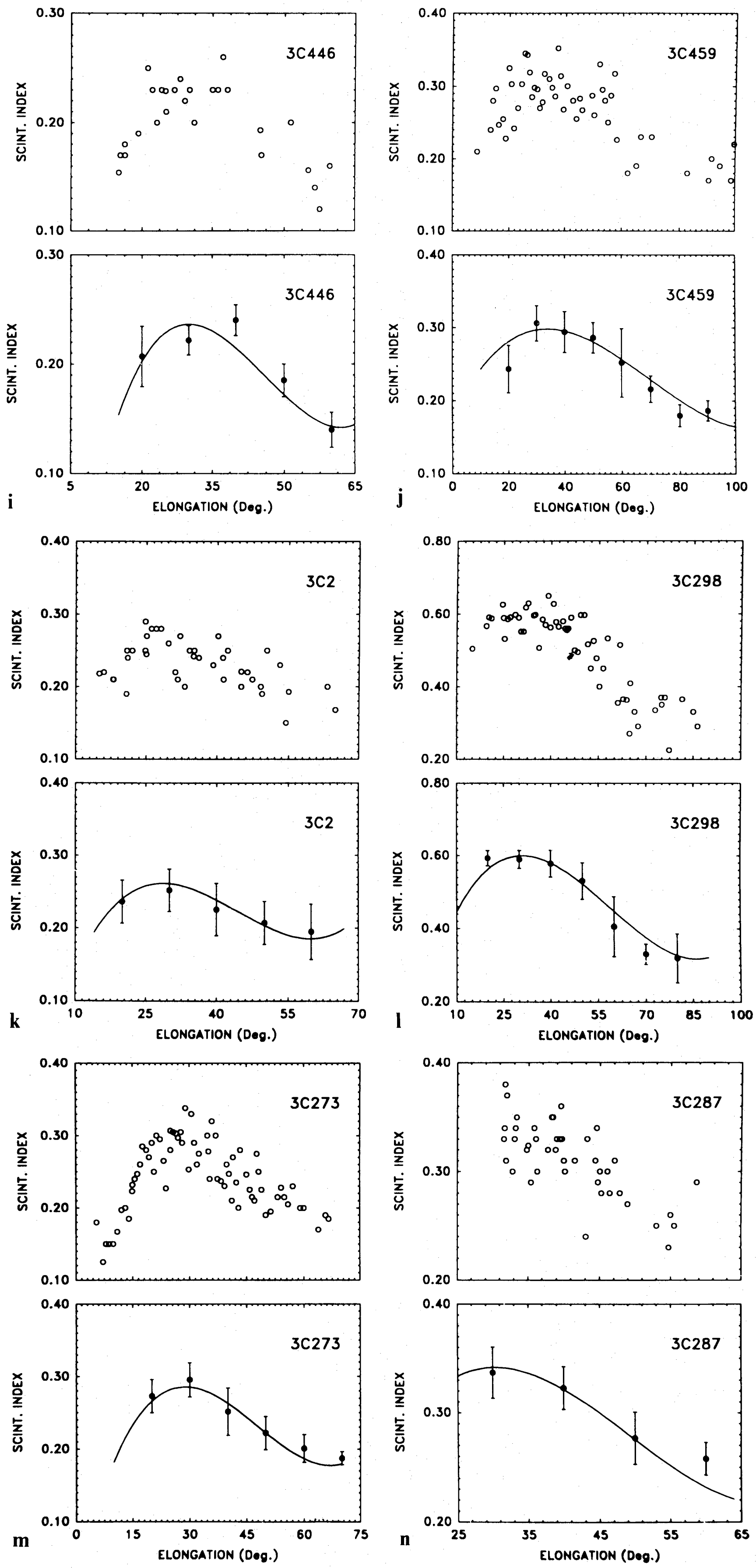

Fig. 5 (continued)

standard error bar in each 10° bin. Now, using the coefficients of the polynomial fit, the ratio, $\mathscr{R}$ of scintillation index at 30° to that at 70° or 30° to that at 60°, as the case may be depending upon the observations, was determined. From these ratios the angular diameter Θ of each of the fourteen sources observed was determined. Table 1 shows the values of source sizes determined at 103 MHz. The source 3C 196 was the weakest scintillator observed and as can be seen from Table 1 it was measured with the least accuracy. Due to the extended period of observations of each source, each set of observations was subject to different observing conditions, signal to noise ratios, interference, solar activity, and varying conditions in the interplanetary medium. Hence all the sources could not be measured with the same accuracies. Table 2 shows the values of source sizes at other frequencies estimated using IPS. The last column shows a few available VLBI measurements at 74 MHz (Resch 1974).

Table 1. Source sizes determined at 103 MHz

Source[a]	Coordinates RA and Dec.	Angular Size Θ″ (103 MHz)	Error Θ″	G. Latitude |b|
3C 119	0429+41	0.72	0.14	4
3C 144	0531+22	0.34	0.10	6
3C 147	0539+50	0.30	0.06	10
3C 48	0135+33	0.35	0.04	29
3C 196	0810+47	0.84	0.27	33
CTA 21	0316+16	0.21	0.04	34
3C 222	0934+06	0.33	0.08	38
3C 237	1005+08	0.58	0.13	47
3C 446	2223−05	0.25	0.05	49
3C 459	2314+03	0.41	0.09	51
3C 2	0004+01	0.49	0.10	61
3C 298	1416+07	0.59	0.07	61
3C 273	1226+02	0.55	0.06	64
3C 287	1328+25	0.45	0.09	81

[a] The sources have been arranged in increasing order of galactic latitude |*b*|.

5. Measurement of interstellar scattering at 103 MHz

Interstellar scattering, as has already been discussed, causes sources to appear larger (Cohen & Cronyn 1974; Rickett 1990) than their true intrinsic size. Angular broadening studies on a sample of 32 radio sources was also carried out using IPS diameter measurements at 81.5 MHz (Readhead & Hewish 1974) and 151.5 MHz (Duffett-Smith & Readhead 1976) to determine the contribution to source broadening at 81.5 MHz. Using the present measurements at 103 MHz and the available diameter measurements at 151.5 MHz a similar study was carried out to determine interstellar broadening at 103 MHz.

The method used is very simple. Any given source can be thought of as having an intrinsic source size Θ_I and an additional component Θ_S which arises due to scattering in the interstellar medium. This can be expressed as

$$\theta_A^2(\nu)=\theta_I^2(\nu)+\theta_S^2(\nu) \quad (3)$$

where Θ_S is the width to $1/e$ of the angular spectrum of the scattered radiation. If Θ_A is measured at two different frequencies ν_1 and ν_2, then we can use equation (1) and the facts that θ_I is independent of frequency and θ_S scales as ν^{-2}

Table 2. Comparison of diameter estimates at different frequencies

Source[a]	IPS–frequency				*VLBI*
	103 MHz	74 MHz	81.5 MHz	151.5 MHz	74 MHz
3C 119	0.72	—	0.35	0.20	—
3C 144	0.34	0.21	—	—	0.18
3C 147	0.30	0.42	0.60	0.30	—
3C 48	0.35	0.41	0.45	0.25	0.32
3C 196	0.84	—	1.20	1.00	—
CTA 21	0.21	—	0.20	0.25	—
3C 222	0.33	—	0.20	0.30	—
3C 237	0.58	0.39	0.40	0.40	0.28
3C 446	0.25	—	0.35	0.10	—
3C 459	0.41	0.48	0.45	0.40	—
3C 2	0.49	—	0.70	0.40	—
3C 298	0.59	0.42	0.40	0.40	0.34
3C 273	0.55	0.44	1.0	0.50	0.37
3C 287	0.45	—	0.35	0.40	—

[a] The sources have been arranged in increasing order of galactic latitude |*b*|.

(Duffett-Smith & Readhead 1976) to write

$$\Theta_A^2(\nu_1)-\Theta_A^2(\nu_2)=\Theta_S^2(\nu_1)-\Theta_S^2(\nu_2)$$
$$=\Theta_S^2(\nu_1)\left[1-\frac{\Theta_S^2(\nu_2)}{\Theta_S^2(\nu_1)}\right]$$
$$=\Theta_S^2(\nu_1)\left[1-\left(\frac{\nu_1}{\nu_2}\right)^4\right]$$
$$\Theta_A^2(\nu_1)-\Theta_A^2(\nu_2)\approx\Theta_S^2(\nu_1) \quad (4)$$

Using Eq. (4) and the measured diameters at 103 MHz (ν_1) and 151.5 MHz (ν_2) the value of Θ_S for each of the sources can be determined. Due to large errors, caused by subtracting two quantities which are themselves uncertain, the apparent 103 MHz diameters are smaller than the 151.5 MHz estimates in some cases. To study the behaviour of Θ_S as a function of galactic latitude, it is therefore necessary to average Θ_S over ranges of galactic latitude. In the present study another difficulty was that the sample of sources available was very small, thereby doing away with the need for any statistical analysis. Figure 6 shows a plot of $(\Theta_S)^2$ as a function of the modulus of galactic latitude for each of the sources. The sources have been marked off into bins of 20°, shown by broken vertical lines, with each value shown by an open circle. The source 3C 196, the weakest scintillator at 103 MHz, has been dropped from this analysis due to its large error. This may be due to the source appearing in the extreme northern beam and due to its large angular size causing scintillations to be reduced. The source 3C 144 does not have a corresponding 151.5 MHz measurement and is also not shown. Figure 7 shows the values of $\langle\Theta_S^2\rangle$ for the four ranges of galactic latitude viz. $|b|\geq 20°$ and $<40°$; $|b|\geq 40°$ and $<60°$; $|b|\geq 60°$ and $<80°$; $|b|\geq 80°$. The solid curve is a best fit to the data beyond 20° using a functional form (Duffett-Smith & Readhead 1976)

$$\Theta_S=\frac{\Theta_0}{(\sin|b|)^{1/2}} \quad (5)$$

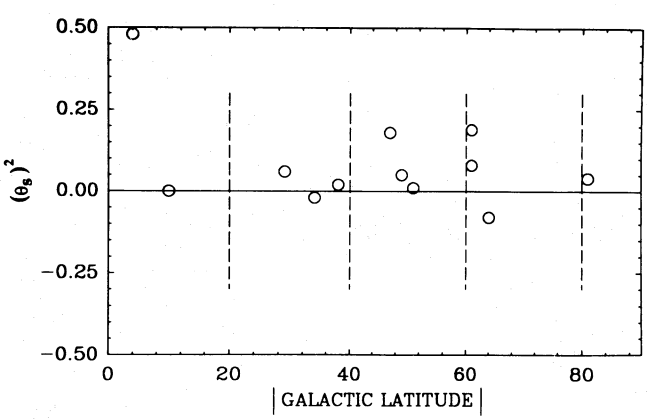

Fig. 6. Shows a scatter plot of the derived values of Θ_S^2 (open circles) as a function of the galactic latitude $|b|$. The vertical broken lines divide the galactic latitude into four ranges of latitude

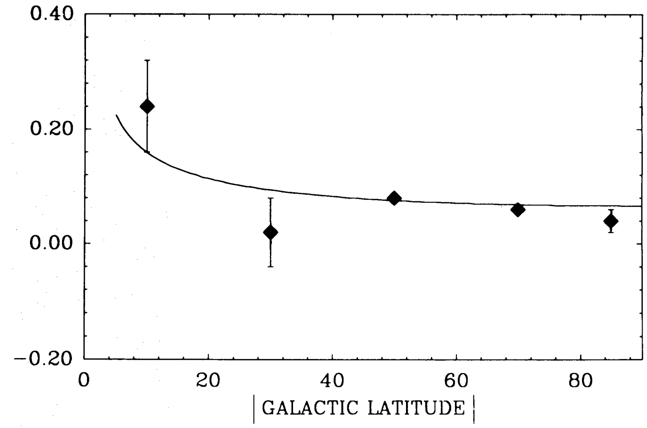

Fig. 7. Shows the values of $\langle\Theta_S^2\rangle$ for the four ranges of galactic latitude. The solid line is a best fit to the data corresponding to $\Theta_0=0.07\pm0.01$ arc seconds for $|b|\geq 20°$

where Θ_0 is a constant. The curve shown in Fig. 7 corresponds to a value of $\Theta_0=0.07\pm0.01$ arc seconds for $|b|\geq 20°$. Thus it can be said that the ISS at 103 MHz amounts to 0.07 ± 0.01 arc seconds for $|b|\geq 20°$. This value compares well with what is expected at this frequency. In a similar study at 81.5 MHz Duffett-Smith and Readhead (1976) derived a value of $\Theta_0=0.15$ arc seconds. Since Θ_S scales as ν^{-2}, one would expect $\Theta_0=0.09$ arc seconds at 103 MHz.

6. Discussion and conclusion

It can be seen from Fig. 5a–n that the polynomial fits show an unrealistic upward trend at large ε due to fewer observations and larger scatter because of contamination by ionospheric scintillation. To avoid the bias caused by this effect, the measurement of ε_2 (see Eq. 1) in the ratio $\mathscr{R}$ was restricted to a maximum of 60° in cases where the polynomial fit showed such a trend. In all other cases ε_2 was measured at 70°. From Table 2 it can be seen that the measured diameter of the source 3C 119 at 103 MHz is much larger than that measured at both 81.5 and 151.5 MHz. This may be due to the very few observations for this source (see Figure 5a) thereby causing the maximum in the polynomial fit to be reduced. Finally, the value of $\Theta_0=0.07\pm0.01$ arc seconds for $|b|\geq 20°$ at 103 MHz could be used as an important correction factor for the source sizes in the determination of solar wind velocities by the single station method (Manoharan & Ananthakrishnan 1990) where the source size is one of the variables in the model calculations.

The measurements of angular diameters of fourteen compact radio sources by the IPS technique at 103 MHz has yielded radio source diameters which are comparable with those at other frequencies and with VLBI measurements where available. The method adopted has been used before by other workers but these are the first measurements at 103 MHz. In spite of having a very small sample of scintillating radio sources the interstellar scattering at 103 MHz has been determined with reasonable accuracy and enhanced scattering due to ISS in the plane of the galaxy has been confirmed.

Acknowledgements. We thank the staff of the Radio Astronomy group for their help and co-operation. We are also grateful to Mr. Krishnakumar C.S. for helping in the scaling of a large number of chart recordings. Financial assistance for this work came from the Departments of Space and Science & Technology, Govt. of India and a Special Foreign Currency (SFC) project No. NA87AA-D-ER046 under Indo–US collaboration.

References

Alurkar S.K., Slee O.B., Bobra A.D., 1986, Aust. J. Phys. 39, 433
Cohen M.H., Gunderman E.J., Harris D.E., 1967, ApJ 150, 767
Cohen M.H., Cronyn W.M., 1974, ApJ 192, 193
Cordes J.M., Weisberg J.M., Boriakoff V., 1985, ApJ 288, 221
Cordes J.M., Weisberg J.M., Frail D.A., Spangler S.R., Ryan M., 1991, Nat 354, 121
Duffett-Smith P.J., 1976, Ph.D. Thesis, University of Cambridge, Cambridge
Duffett-Smith P.J., Readhead A.C.S., 1976, MNRAS 174, 7
Harris D.E., Zeissig G.A., Lovelace R.V., 1970, A&A 8, 98
Kaufmann J.J., 1976, Ph.D. Thesis, University of California, San Diego
Kemp M.C., 1979, Ph.D Thesis, University of Cambridge, Cambridge
Kemp M.C., 1979, Ph.D Thesis, University of Cambridge, Cambridge
Little L.T., Hewish A., 1966, MNRAS 134, 221
Manoharan P.K., Ananthakrishnan S., 1990, MNRAS 244, 691
Marians M., 1975b, Radio Sci. 10, 115
Purvis A., 1981, Ph.D. Thesis, University of Cambridge, Cambridge
Rao A.P., Bhandari S.M., Ananthakrishnan S., 1974, Aust. J. Phys 27, 105
Readhead A.C.S., 1971, MNRAS 155, 185
Readhead A.C.S., Hewish A., 1972, Nat 236, 440
Readhead A.C.S., Hewish A., 1974, Mem. R. Astron. Soc. 78, 1
Readhead A.C.S., Kemp M.C., Hewish A., 1978, MNRAS 185, 207 (RKH)
Resch G.M., 1974, Ph.D. Thesis, Florida State University
Rickett B.J., 1990, ARA&A 28, 561